Spatial variations in paleowind direction during the last glacial period in north China reconstructed from variations in the anisotropy of magnetic susceptibility of loess deposits

Junyi Ge [a,b,c,*], Zhengtang Guo [b], Deai Zhao [b], Ying Zhang [d], Tao Wang [d], Liang Yi [e], Chenglong Deng [e]

[a] Key Laboratory of Vertebrate Evolution and Human Origins of the Chinese Academy of Sciences, Institute of Vertebrate Paleontology and Paleoanthropology, Chinese Academy of Sciences, Beijing 100044, China
[b] Key Laboratory of Cenozoic Geology and Environment, Institute of Geology and Geophysics, Chinese Academy of Sciences, Beijing 100029, China
[c] State Key Laboratory of Paleobiology and Stratigraphy, Nanjing Institute of Geology and Paleontology, Chinese Academy of Sciences, Nanjing 210008, China
[d] Nansen-Zhu International Research Centre, Institute of Atmospheric Physics, Chinese Academy of Sciences, Beijing 100029, China
[e] State Key Laboratory of Lithospheric Evolution, Institute of Geology and Geophysics, Chinese Academy of Sciences, Beijing 100029, China

ARTICLE INFO

ABSTRACT

Anisotropy of magnetic susceptibility (AMS) of Chinese loess is considered to be an effective tool for determining paleowind direction. However, the relationship between AMS and the paleowind direction is still a matter of debate. This study reports the results of AMS measurements of Chinese loess deposited during the last glacial period on slopes of varying slope angles and orientations. The sites are located on the Chinese Loess Plateau, in West Qinling, and on the eastern margin of Qilian Mountain. The results show that within the same region, magnetic lineations are clustered along similar orientations despite differences in slope exposure and slope angle, but that different regions exhibit different directions of magnetic lineation. These results suggest that the alignment of the magnetic grains during deposition of the eolian deposits was determined by air circulation rather than by water flow on the surface of the slopes, and therefore that the AMS of Chinese loess can be used to determine paleowind directions. In addition, our results indicate that the AMS of Chinese loess is determined mainly by the patterns of regional surface wind flow that occurred during dust accumulation rather than by the uniform pattern of large-scale atmospheric circulation. In addition, since wind direction is influenced significantly by regional topography, the AMS of Chinese loess may have the potential to detect significant changes in past regional topography.

© 2014 Elsevier B.V. All rights reserved.

1. Introduction

The spatially correlative Quaternary loess–soil sequences in the Chinese Loess Plateau, characterized by alternations of loess and paleosol layers, have long been considered to preserve some of the most detailed long-term records of changes in East Asian monsoon climate during the Quaternary (Liu, 1985). Moreover, the oldest loess–soil sequences have been dated back to the early Miocene or late Oligocene (Guo et al., 2002; Qiang et al, 2011). Generally, during cold/dry glacial periods, eolian dust was transported from northern source areas by the winter monsoon and deposited on the Chinese Loess Plateau, while during warm/humid interglacial periods eolian inputs decreased dramatically and paleosol formation was promoted by the

increased precipitation generated by an enhanced summer monsoon (An et al., 1990; Liu, 1985). Given its relationship with patterns of monsoonal air circulation, the Chinese loess is also regarded as having the potential to provide records of paleowind direction on the Chinese Loess Plateau (e.g. An et al., 1991; Ding et al., 1995; Guo et al., 2000; Liu and Ding, 1998).

The anisotropy of the low-field magnetic susceptibility (AMS) is a rapid and precise tool for determining the fabric of rocks and sediments by quantifying the average preferred crystallographic and dimensional (or shape) orientations of magnetic grains (e.g. Tarling and Hrouda, 1993). Since loess deposits are accumulations of windblown dust, the AMS of loess is a sensitive indicator of the texture of the magnetic fabric generated by patterns of wind flow, and thus wind directions can potentially be inferred from AMS measurements.

The first AMS study on Chinese loess was done by Heller et al. (1987), and demonstrated that loess at the Luochuan section exhibited a uniform magnetic fabric and sedimentation rate through time. Later, Liu et al. (1988) suggested that AMS parameters could be used to evaluate the re-working of wind-blown sediments by water. Subsequently,

Thistlewood and Sun (1991) revealed that the maximum axes of the AMS ellipsoids in both loess and paleosol samples from a cross section in loess near Xi'an were uniformly distributed along the WNW–ESE direction, and they suggested that AMS of loess may indicate the direction of the prevailing paleowind near ground level. This relationship between wind direction and the orientation of K_{max} (where K_{max} and K_{min} are the maximum and minimum principal axes of the AMS ellipsoid, respectively) was later confirmed by wind-tunnel experiments, which demonstrated a strong correlation with deviations less than 20° (Wu et al., 1998). Subsequent AMS studies on loess sequences in central Alaska (Lagroix and Banerjee, 2002, 2004), Poland and Ukraine (Nawrocki et al., 2006), Hungary (Bradák, 2009) and China (Huang and Sun, 2005; Liu et al., 2008; Sun et al., 1995; Wang et al., 2007) confirmed this correlation. For example, the AMS of the Alaskan loess faithfully records eolian transportation directions, which are associated with major paleoclimatic changes over the Alaskan region: the recorded wind direction shifted from a NW–SE to N–S direction from glacial to interglacial periods, respectively (Lagroix and Banerjee, 2002).

However, despite the foregoing there are still areas of disagreement about the relationship between AMS and the paleowind direction. For example, the work of Zhu et al. (2007) indicated that K_{max} is chaotically distributed and cannot be used to determine paleowind directions at three loess profiles on the Chinese Loess Plateau; and similar phenomena were observed in loess–soil sequences at Kurtak in Siberia (Zhu, 2000), and at Luochuan in the Chinese Loess Plateau (Liu and Sun, 2012). In addition, in the case of the youngest loess deposits in Poland and Ukraine, it was concluded that the orientation of K_{max} did not reflect the prevailing paleowind directions (Nawrocki et al., 2006). Therefore these results seem to cast doubt on the fidelity of the AMS of loess as an indicator of paleowind direction.

Even in those studies in which consistent K_{max} orientations are observed there has still been debate about their interpretation. According to AMS studies on the loess in China (Huang and Sun, 2005; Liu et al., 2008; Sun et al., 1995; Wang et al., 2007), Alaska (Lagroix and Banerjee, 2002, 2004) and Hungary (Bradák, 2009), the orientation of K_{max} mainly reflects the transportation direction of eolian dust. Therefore in China the East Asian winter monsoon, which transports dust from northwestern desert areas, was considered to be responsible for the development of magnetic fabric in loess sequences. However Zhu et al. (2004) demonstrated that in the area southeast of the Liupan Mountains, the K_{max} of AMS is orientated in the NE–SW and NW–SE directions during glacial and interglacial intervals, respectively. The authors interpreted these results in terms of dust transport by the NE winter monsoon and moisture transport by the SE summer monsoon. Recently, Zhang et al. (2010) examined the AMS of three loess sections along an east–west transect in the Chinese Loess Plateau, and their results suggested that the East Asian summer monsoon, rather than the winter monsoon, played the dominant role in generating the imbrication of the magnetic grains and thus the development of the AMS.

In the present study, we firstly made AMS measurements of loess deposited during the last glacial period at six sections near Luochuan, central Chinese Loess Plateau. Samples were obtained from paleo-slopes with different slope azimuths and dip angles in order to test the ability of the AMS of the loess consistently to reflect the paleowind direction within a particular area. Subsequently we studied an additional four loess sections from various regions, including those on the Chinese Loess Plateau, in the West Qinling, and on the eastern margin of Qilian Mountain, and compared the results with those of previous studies, in order to provide additional insights into the climatic implications of the AMS of the Chinese loess.

2. Sampling and methods

The Chinese loess unit of the last glacial, L_1, is the eolian deposit most widely distributed in north China. It is yellowish in color and massive in structure, and can generally be subdivided into five sub-units, termed L_{1-1}, L_{1-2}, L_{1-3}, L_{1-4} and L_{1-5}. L_{1-2} and L_{1-4} are weakly developed soils, and the others are typical loess horizons. Previous studies (Ding et al., 2002; Kukla, 1987; Lu et al., 2007) have shown that L_{1-1} is correlated with MIS 2, L_{1-5} with MIS 4 and L_{1-2}, L_{1-3} and L_{1-4} collectively with MIS 3. The L_1 loess is generally overlain by the Holocene soil, S_0, which is dark in color because of its relatively high organic matter content. Due to its rapid accumulation rate, the Chinese loess of the last glacial can be observed mantling deposits of differing ages and deposited on different geomorphological units, including the Chinese Loess Plateau and its surrounding mountains, and some alluvial flood plains. In addition, because the Holocene soil S_0 has typically been disturbed by agricultural activity, the last glacial loess is frequently exposed and constitutes most of the ground surface across the Chinese Loess Plateau and can be easily recognized in the field.

In this study, 10 loess sections of the last glacial on different paleo-slopes at different sites were studied (Fig. 1), including sites on the Chinese Loess Plateau, in the West Qinling, and on the eastern margin of Qilian Mountain. A total of 1107 block samples, oriented by magnetic compass in the field, were collected. The azimuths and dip angles of these paleo-slopes, where the loess was deposited during the last glacial period, as observed within the Luochuan (LC1, LC2, LC3, LC4) and Tongchuan (TC1) sections, can be defined by the underlying paleosol layers the parent material of which was usually formed by depositional processes and controlled by the local paleotopography. These angles are 115°∠14°, 140°∠30°, 60°∠24°, 40°∠20° and 240°∠13°, respectively; and those of the other sections, including Xihe, Dongwan, Xining and Tianzhu, are horizontal. In the laboratory, cubic specimens of 2-cm edge length were cut for AMS measurements.

Various techniques were used to determine the magnetic mineralogy of representative samples from these sections. Hysteresis loops were measured using a Princeton MicroMag 3900 Vibrating Sample Magnetometer (VSM) with a maximum magnetic field of 1 T. Saturation magnetization (M_s), saturation remanence (M_{rs}) and coercivity (B_c) were determined after correction for the paramagnetic contribution. Samples were then demagnetized in alternating fields (AFs) up to 500 mT and isothermal remanent magnetizations (IRMs) were imparted from 0 to 1.0 T, also using the MicroMag 3900 VSM. Subsequently, the saturation isothermal remanent magnetization (SIRM) (the IRM acquired at the maximum field of 1.0 T) was demagnetized in a stepwise direct current backfield in order to obtain the coercivity of remanence (B_{cr}).

The AMS of each sample was measured using a KLY-3S Kappabridge (Agico Ltd., Brno) with an automated sample handling system. Each sample was rotated through three orthogonal planes. The susceptibility ellipsoid was calculated using the least-squares method, and the anisotropy parameters of lineation (L), foliation (F), degree of anisotropy (P), and shape factor (T) (Jelinek, 1981) were obtained with Anisoft software using the statistical method of Constable and Tauxe (1990). All the experiments were performed in the Paleomagnetism and Geochronology Laboratory of the Institute of Geology and Geophysics, Chinese Academy of Sciences.

3. Results

3.1. Magnetic properties

After the removal of the paramagnetic contribution, hysteresis loops for most of the samples are almost closed above 0.3 T (Fig. 2a–f), which is consistent with the presence of a dominant ferrimagnetic phase (e.g., magnetite, maghemite). The IRM curves for most of the samples rise rapidly below 0.1 T and reach approximate saturation at about 0.3 T (Fig. 2g), which confirms the abundance of low-coercivity ferrimagnetic minerals such as magnetite and/or maghemite. The stepwise demagnetization of SIRM using a DC backfield also shows a moderately low coercivity of remanence (B_{cr}) for all samples, consistent with ferrimagnetic carriers (Fig. 2h). In the Day plot (Day et al., 1977), all samples
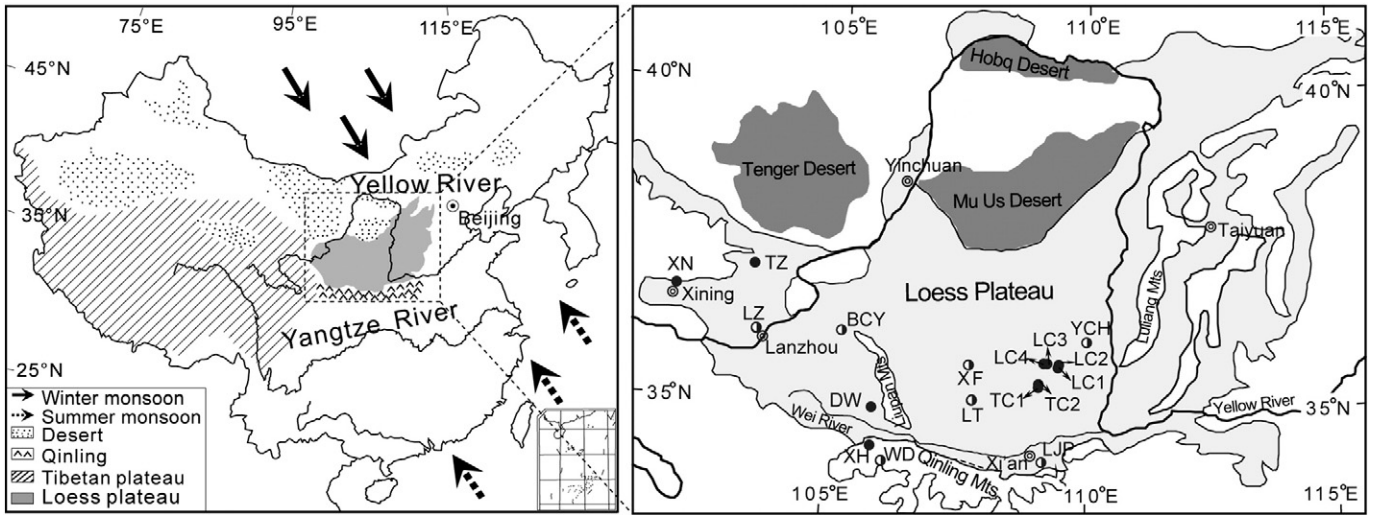
Fig. 1. Location of the sampling sites discussed in the text. Solid (half shaded) circles represent the newly measured (published) sections. The codes of sections and cities are as follows: BCY, Baicaoyuan; DW, Dongwan; LC, Luochuan; LJP, Liujiapo; LT, Lingtai; LZ, Lanzhou; XF, Xifeng; XH, Xihe; TC, Tongchuan; TZ, Tianzhu; XN, Xining; WD, Wudu; YCH, Yichuan.

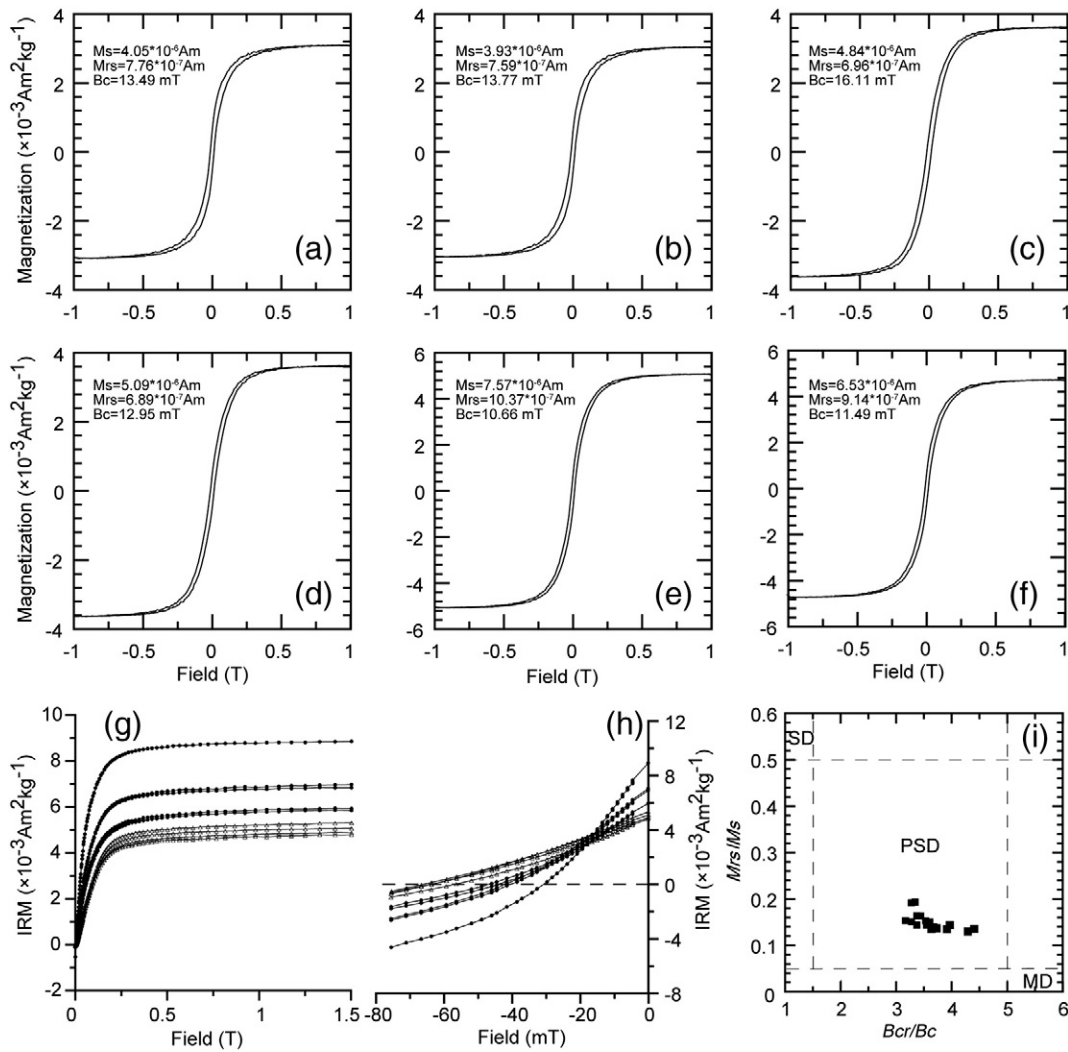**Fig. 2.** Mineral magnetic properties for representative samples. (a–f) Hysteresis oops after slope correction for the paramagnetic contribution. The hysteresis loops were measured in fields up to ± 1.0 T. (g) Isothermal remanent magnetization (IRM) acquisition curves. (h) Back-field demagnetization of IRM. (i) Hysteresis ratios plotted on a Day plot (Day et al., 1977). SD, single domain. PSD, pseudo-single domain. MD, multidomain.

are almost indistinguishable, in the pseudo-single-domain (PSD) range (Fig. 2i). These results are rather consistent with those of previous studies (Deng et al., 2004; Fukuma and Torii, 1998; Ge et al., 2012; Liu and Sun, 2012).

3.2. AMS results

The AMS of a sample can be described in terms of an ellipsoid with three orthogonal principal axes corresponding to the maximum, inter-mediate, and minimum principal (K_{max}, K_{int} and K_{min}) axes, respectively. The major AMS parameters (Tarling and Hrouda, 1993) examined in this study are as follows:

$$\text{lineation } (L) = K_{max}/K_{int}, \tag{1}$$

$$\text{foliation } (F) = K_{int}/K_{min}, \tag{2}$$

$$\text{degree of AMS } (P) = K_{max}/K_{min}, \tag{3}$$

and the shape parameter of AMS $(T) = (2\eta 2 - \eta 1 - \eta 3)/(\eta 1 - \eta 3)$, (4)

where $\eta 1$, $\eta 2$ and $\eta 3$ are $\ln(K_{max})$, $\ln(K_{int})$ and $\ln(K_{min})$, respectively.

In the studies of Zhu et al. (2004), parameters F_{12} and F_{23} were usually used to evaluate the statistical significance of the lineation and the foliations, and in general values larger than 4 were taken to indicate statistically significant anisotropies. E_{12} represents the half-angular uncertainty in the direction of K_{max} within the magnetic foliation plane. Because the measured foliation is generally almost horizontal, E_{12} represents the 95% confidence angle for the azimuth of K_{max} and the measurement with $E_{12} < 22.5°$ is considered to satisfy the statistically significant level (Lagroix and Banerjee, 2004; Zhu et al., 2004). In these notations, 1, 2 and 3 are assigned to K_{max}, K_{int} and K_{min}, respectively.

The majority of samples from all studied localities have statistically significant magnetic lineations and foliations, with $F_{12} > 4$, $E_{12} < 22.5°$

and $F_{23} > 10$ (Fig. 3a–c). As shown in Fig. 3d, an inverse relationship between E_{12} and the magnetic lineation parameter L can be observed in all sections, probably due to the increasing random measurement errors for K_{max} in the lineation plane with weaker lineation. To eliminate noisy directions, 114 samples of measurements with $F_{12} < 4$ or $E_{12} > 22.5°$ were rejected (as indicated by the shaded area in Fig. 3a).

The principal AMS parameters for most of the samples show a degree of anisotropy (P) between 1 and 1.061 (Fig. 3e). The anisotropy shows a high degree of positive correlation with the magnetic foliation, indicating that anisotropy is determined by foliation (Fig. 3e). In an L–F diagram, the samples lie close to the foliation axis, and the shape param-eter (T) of the AMS ellipsoids is also generally located in the oblate area, as shown in Fig. 3f, indicating that the AMS ellipsoid of the samples is oblate. These results are consistent with those of previous studies (Lagroix and Banerjee, 2004; Liu and Sun, 2012; Zhu et al., 2004), and indicate a primary eolian magnetic fabric without significant disturbance.

The K_{min} directions are described by the inclination (Inc-K_{min}) and declination (Dec-K_{min}) of K_{min} distributed along the vertical axis of the stereonet projection. Inc-K_{min} is greater than 70° in 95.5% of all samples from these ten sections, corresponding to an undisturbed (less reworked) loess with an observed oblate fabric.

Fig. 4 and Table 1 illustrate the principal orientations of the mini-mum and maximum susceptibility axes. In the LC1, LC2, LC3, and LC4 sections from Luochuan, the minimum magnetic susceptibility direc-tions of all samples are tightly vertical without significant deviation, and are independent of the variations of the dip angles of these sections from 13° to 30°. Similar observations are valid for the samples from the TC1 and TC2 sections near Tongchuan, 110 km south of Luochuan. Regardless of slope angle, samples from the two sections show similar average Inc-K_{min} values of 81.9 ± 2.7° and 84.0 ± 3.2°. These results indicate that the AMS of eolian dust is not significantly influenced by changes of paleo-topography, and are undisturbed. In all the sections studied, the maximum susceptibility axes of the samples are all clus-tered along a specific direction. For all of the six sections from Luochuan and adjacent Tongchuan, K_{max} has the majority of samples oriented along the NE–SW direction (Table 1), irrespective of the inclination of the slope bedding. In the case of the Xining, Tianzhu, Dongwan, and
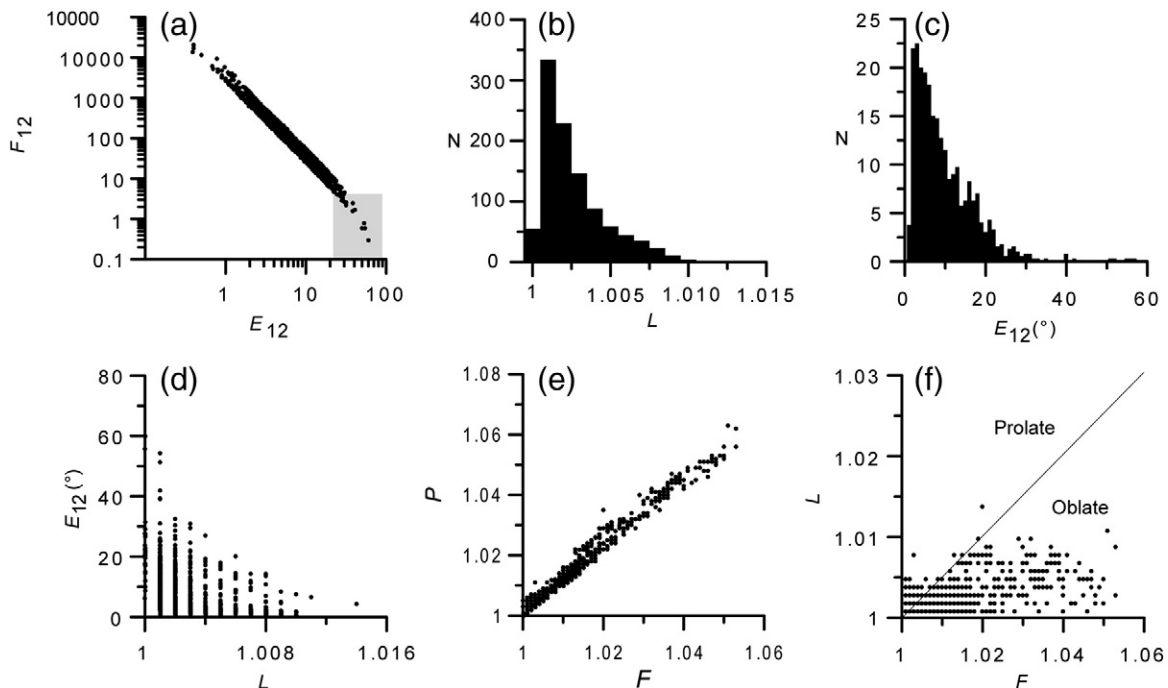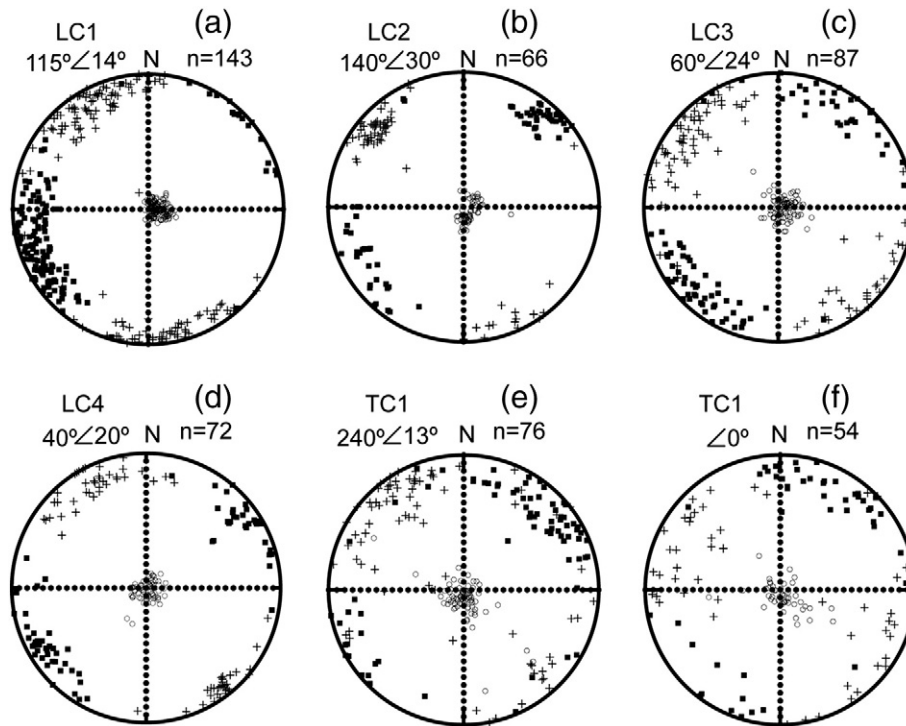

Fig. 3. Statistical significance, angular uncertainties and relationships between the AMS parameters. The shaded area corresponds to samples with $F_{12} < 4$ and $E_{12} > 22.5°$.

Fig. 4. Equal-area projections of AMS principal axes of samples from six sites near Luochuan (LC) and Tongchuan (TC) having underlying paleosols with different slopes. Squares, crosses and circles represent K_{max}, K_{int} and K_{min}, respectively. The numbers, i.e., "115°∠14°", correspond to the slope azimuths and dip angles of the paleo-slopes in these sections, respectively. The directions are plotted in geographic coordinates without correction for the slope of the underlying paleosol. The projections are all in the lower hemisphere.

Xihe sections, the K_{max} directions are biased towards NW–SE (D-K_{max} = 333.4°), NW–SE (D-K_{max} = 144.7°), NE–SW (D-K_{max} = 13.1°) and near E–W (D-K_{max} = 86.9°), respectively (Fig. 5 and Table 1). The results of the Xining section in this study are rather consistent with previous studies (Zhang et al., 1993).

4. Interpretation and discussion

The AMS of a sediment is largely determined by gravitational, hydrodynamic and magnetic forces, and consequently by the size, shape and mass of the detrital grains (Tarling and Hrouda, 1993). In addition, topography, weathering, bioturbation, and the types of magnetic minerals also play important roles in the formation of the AMS (Ellwood, 1984; Rees et al., 1968).

In the case of very fine-grained (mostly < 1–2 μm), strongly magnetic particles settling in quiet conditions, magnetic forces may promote a lineation result in the bedding plane as the direction of the longest

Table 1
Mean direction and corresponding statistical parameters for all studied sections using Bootstrap statistics (Constable and Tauxe, 1990).

Section	N	K_{max}		K_{int}		K_{min}	
		D/I	$E_1//E_2$	D/I	$E_1//E_2$	D/I	$E_1//E_2$
LC1	143	246.3/6.8	4.9/1.0	336.7/2.7	4.9/1.3	86.3/82.6	1.3/1.1
LC2	66	44.6/2.2	3.6/1.9	314.3/7.5	3.0/1.3	150.9/82.2	2.5/1.2
LC3	87	222.2/2.5	6.4/3.2	312.4/4.7	6.1/5.4	94.2/84.7	4.0/2.2
LC4	72	56.1/1.5	5.7/3.7	326.1/1.1	4.8/1.8	199.4/88.1	3.1/1.9
TC1	76	46.9/5.2	6.7/2.7	316.3/6.1	6.8/3.9	181.2/81.9	2.7/4.1
TC2	54	29.2/3.8	14.0/3.3	298.9/4.7	13.5/4.6	158.5/84.0	3.2/4.7
DW	212	13.1/0.5	15.5/5.3	283.1/2.1	8.3/1.6	117.4/87.8	1.3/2.2
LC	368	232.2/2.1	2.6/1.1	322.4/4.7	2.5/1.0	117.7/84.8	1.3/0.9
TC	130	42.5/4.8	6.1/2.1	312.0/5.5	6.1/2.9	173.0/82.7	2.2/2.9
TZ	124	144.7/9.7	5.3/1.4	236.9/12.9	5.3/1.5	288.7/81.1	1.6/1.3
XH	55	86.9/1.7	19.2/2.0	176.9/1.4	19.2/1.8	306.4/87.8	1.9/1.7
XN	104	333.4/6.4	10.9/2.9	243.1/2.9	12.0/4.3	129.3/83.0	3.8/2.9

axes of rod-like magnetic particles will be biased towards the field direction (Hus, 2003). While gravitational forces dominate, the majority of the platy grains will settle on the bedding plane and this will result in an oblate fabric confined to the bedding plane, with the minimum shape axis perpendicular to the bedding plane (Hus, 2003). In all the sections examined, lineation is low and evidence of field alignment in AMS is lacking, even though magnetite and/or maghemite grains are abundant. Indeed, the influences of magnetic force have been shown to be negligible, especially in the case of the AMS of loess (Hus, 2003; Wu and Yue, 1997). Most of the samples are characterized by an oblate fabric, with low lineation and relatively high degree of foliation, as well as by the tight grouping of the K_{min} directions along the perpendicular to the bedding plane, reinforcing the fact that gravitational force determines the magnetic fabric and thus indicating a primary depositional fabric.

During weathering and soil formation, the loess microfabric will become less open due to redistribution of fines and by authigenesis, and the original fabric will also be affected by bioturbation. In this study, however, the effects of weathering and bioturbation may be almost negligible, because a large amount of evidence has shown that in the study region the last glacial was cold and dry, with low weathering and pedogenic intensity, sparse vegetation cover and weak biological activity (Guo et al., 1991; Liu, 1985).

Hydrodynamic force is considered to be a major influence on the grain orientation that yields the magnetic fabric, especially in the case of magnetite and maghemite grains in which the AMS is usually controlled by particle shape where the maximum susceptibility axis is parallel to the grain's long dimension in coarse-grained (pseudo-single, PSD, and multi-domain, MD) particles (Rees et al., 1968; Hrouda, 1993). According to Tarling and Hrouda (1993), when deposition occurs in still water, gravitational settling is the only significant force and the majority of rod-like ferrimagnetic grains are arranged with their longer axes aligned randomly within the bedding plane. Under a weak water current, most elongated magnetite grains line up parallel to the current direction and the superposition of gravity and current forces causes most of the maximum AMS axes to tilt in the upstream direction and the
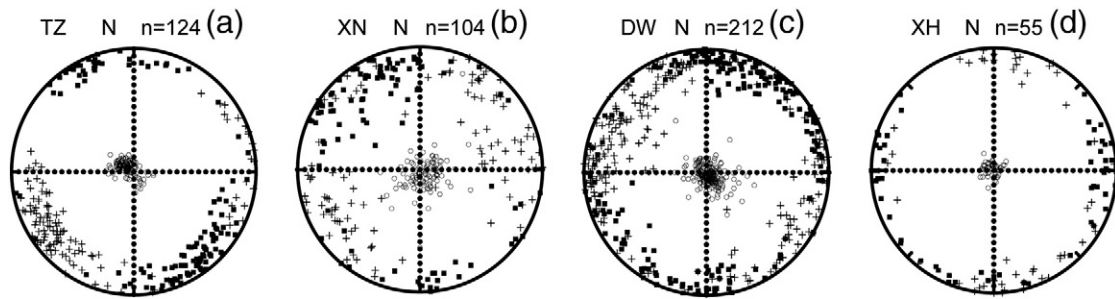
Fig. 5. Equal-area projections of AMS principal axes of the samples from Tianzhu (TZ), Xining (XN), Wudu (DW), and Xihe (XH) sites. Squares and circles represent K_{max} and K_{min}, respectively. The projections are all in the lower hemisphere.

minimum axes (K_{min}) to tilt in the downstream direction. The prolate grains are more stable when their longest axes lie perpendicular to the direction of water flow. The stronger the current, the higher the tendency of prolate particles to become oriented perpendicular to the current flow.

When sloping depositional surfaces are present during deposition, a magnetic fabric very similar to that produced by deposition from running water onto a horizontal bed will be produced, especially in the case of rod-like magnetic mineral particles. Rees (1966) found that when the angle of slope of the bed approaches the angle of rest of the sediment, the slope-deposited sediments usually have a preferred long-axis orientation which is tilted downslope. Currents depositing materials on a slope will form sediments with magnetic fabrics whose linear and planar components tend to reflect the directions of both current flow and slope (Tarling and Hrouda, 1993).

In the case of eolian dust deposited on beds of different inclination and dip angle, if the AMS was determined by water flow on the beds, which is in a similar direction to the inclination of the slope beddings, we would expect a maximum susceptibility axis oriented along the direction of the flow and the minimum susceptibility axis tilted in the same direction. However, our results show that in the case of the six sections from Luochuan and nearby Tongchuan, the K_{max} of the majority of samples is oriented along the NE–SW direction, irrespective of the orientation of the direction of slope. This indicates that neither the overland flow nor the orientation of the direction of slope determines the AMS of the loess of the last glacial period in north China. Wind tunnel experiments (Wu et al., 1998) have also demonstrated that eolian deposition is analogous to deposition under hydrodynamic conditions. Therefore we conclude that the wind force is mainly responsible for the formation of the magnetic fabric, otherwise it would not produce a uniform AMS over such a large area. Our results thus provide independent evidence that eolian processes determine the AMS of Chinese loess and confirm the utility of AMS measurements for determining the paleowind direction.

Early studies on the AMS of Chinese loess (Huang and Sun, 2005; Liu et al., 2008; Sun et al., 1995; Thistlewood and Sun, 1991; Wang et al., 1995; Zhong et al., 1996) showed a maximum susceptibility axis orientation mainly along the NW–SE direction. Given the similarity of the direction of the East Asian Winter Monsoon circulation and the results of wind tunnel experiments (Wu et al., 1998), these authors suggested that the winter monsoon flow, coming primarily from the northwestern central Asian desert areas and carrying the majority of the sedimentary particles, determines the orientation of the magnetic fabric in both loess and paleosol horizons. Recently, Zhang et al. (2010) examined the AMS of three loess sections along an east–west transect in the Chinese Loess Plateau. Although the AMS of these sections all show a NW–SE orientation, they argued that it is the East Asian summer monsoon which is mainly responsible for the formation of the AMS. It is noteworthy that in the case of the Lingtai loess section, Zhu et al. (2004) found that the K_{max} of the AMS was distributed along the NE–SW and NW–SE directions during glacial and interglacial intervals, respectively. They

concluded that these results reflected dust transport by the NE winter monsoon and moisture transport by the SE summer monsoon.

However our results demonstrate that at Luochuan and Tongchuan the K_{max} of the AMS is distributed along a NE–SW axis, while in the Tianzhu, Xining, Dongwan and Xihe areas it is oriented along NW–SE, NE–SW and E–W axes, respectively (Fig. 4). Our results thus indicate that there are significant regional differences in paleowind directions estimated by AMS measurements of the last glacial loess in north China. To further investigate this finding, we examined the AMS results from seven other loess sections spanning the last glacial period from Xifeng (Zhang et al., 2010), Baicaoyuan (Zhang et al., 2010), Yichuan (Zhang et al., 2010), Lingtai (Zhu et al., 2004), Wudu (Wang et al., 1995), Lanzhou (Clarke, 1995; Wang et al., 1995), and Xi'an (Thistlewood and Sun, 1991). We found that the K_{max} of AMS in these areas was also clustered in different directions: NW–SE in Xifeng, Baicaoyuan, and Yichuan; NE–SW in Lingtai; and E–W in Wudu and Lanzhou (Fig. 6). Therefore, these results further confirm our conclusions and suggest that the AMS in these eolian deposits corresponds to regional surface winds, whose directions are determined not only by the monsoon circulation but also by the regional topography and thus somewhat different from the mean direction of the large-scale monsoon circulation.

In north China, the climate is characterized by the waxing and waning of the East Asian monsoon circulation. In winter (December, January and February) and spring (March, April, May), the northerly wind comes from the northwestern central Asian desert and carries a majority of the dust particles; while in summer (June, July and August), the southerly wind carrying precipitation from the southeast ocean areas prevails (Chen et al., 1991). However, as shown in Fig. 6, due to the influence of the high mountains in north China, especially of the Tibetan Plateau, the surface wind flow in both summer and winter is deflected in the area of the Chinese Loess Plateau and West Qinling. For example, the direction of winter surface wind in the Xi'an and Xihe areas shifts from NW–SW to NE–SW and E–W, respectively. In addition, the regional orography also promotes significant variability in wind directions: for example, in the Lanzhou area, the surface wind direction is mainly NE–SW throughout the year due to the significant impact of the NE-oriented Yellow River valley (Liu, 1998).

Next we compare our results with the present day regional surface wind directions compiled using online publically available data from the European Centre for Medium-Range Weather Forecasts (ECMWF) ERA-Interim Reanalysis data (Dee et al., 2011). Surface wind directions and speed for the winter and spring months of December–May when the dust storms mainly takes places and the summer months of June–August are calculated from the 1979 to 2012 monthly means. Modern summer surface wind in the study areas is dominantly from the southeast and shows an anticlockwise rotation in the proximity of the Southeast Tibetan Plateau. The winter surface wind is obviously controlled by the regional orography and shows much greater variability in direction in comparison with the summer wind (Fig. 6). In the desert areas to the north of the Chinese Loess Plateau, the winter surface wind

Fig. 6. AMS results of Chinese loess of the last glacial period and comparison with the surface wind vectors for (a) the summer months of June–July–August and (b) the winter and spring months of from December to May calculated from the 1979 to 2012 monthly long-term means. Data was compiled by the ECMWF ERA-Interim Reanalysis Atlas (Dee et al., 2011). Contours are wind velocities in meters per second. White (black) stars represent the newly measured (published) sections. Figures of BCY, XF, YCH and LT sections are from Zhang et al. (2010) and Zhu et al. (2004), while AMS results of LZ, WD and LJP sections are from Wang et al. (1995), respectively. See the caption of Fig. 1 for acronyms of the sections. Contour lines of the stereonet projections were constructed by following the computing method of Robin and Jowett (1986). In the Rose diagrams of K_{max}, the stereonets are split into an equal number of 10° segments.

is strong enough (>2 m/s) to carry the dust particles towards the south. In contrast in the Loess Plateau area, the wind strength in winter is significantly weaker and results in significant dust deposition. At most of the studied sites (Fig. 6), the paleowind directions inferred from the AMS are rather consistent with the regional modern winter surface wind. However, they are significantly different from those which were obtained during the summer monsoon, especially in the case of the sites in areas to the south and northwest of the Chinese loess Plateau, such as at Xihe, Wudu, Dongwan, Lanzhou and Tianzhu.

The magnetic fabric of eolian deposits is imparted by the combination of gravity and surface wind forces. During the course of deposition on the ground surface, dust particles (and magnetic grains) are oriented by the surface wind. As they are buried by fresh eolian deposition, the particles are fixed and finally immobilized with the help of the vegetation and by precipitation. Because the majority of the eolian dust is transported and deposited in the winter and spring in the Chinese Loess Plateau, the alignment and orientation of the magnetic minerals (magnetite and/or maghemite) in the loess are mainly determined by the winter surface wind, consistent with the results of wind tunnel experiments and laboratory simulation experiments, as well the field observations (Wu et al., 1998). Similar observations have been reported in the Daluliang loess section in Shanxi Province in north China (Liu

et al., 2013). Here it was found that the paleowind direction inferred from AMS measurements remained unchanged during the past 0.9 myr, consistent with the strike of the Jinshan (i.e. Shanxi and Shaanxi) gorge where the surface wind is obviously restricted by the gorge.

It is clear that there inevitably are uncertainties in using modern climatic data to examine the climatic implications of the loess AMS; nevertheless Mock et al. (1998) have argued for the usefulness of modern synoptic climatology as a conceptual guide to test paleoclimatic hypotheses. Meanwhile, the spatial variations of grain size (Yang and Ding, 2008) and magnetic susceptibility (Hao and Guo, 2005; Sun et al., 1996) of Chinese loess have also demonstrated that the directions of the East Asian monsoons have remained virtually unchanged since the last glacial period. In addition, the regional topography in north China, which controls the surface wind direction, does not seem to have changed significantly from the last glacial period to the present (CLIMAP, 1976). Therefore we conclude that the present pattern of surface wind flow in the studied areas can reliably be used for comparison with the last glacial period.

The vegetation cover and precipitation intensity also affect the orientation of magnetic particles on the ground. Generally, the sedimentary grains will be reoriented if they are temporarily intercepted by vegetation before reaching the ground surface. Similarly, any overland flow resulting from heavy precipitation could also lead to the reorientation of the sedimentary particles. In the winter and spring seasons, much of the semi-arid and/or arid zones in north China is dominated by sparse grassland. In addition, the precipitation here is usually quite low (<0.4–0.9 mm/d) in these two seasons and is easily absorbed by the dry and porous loess, inhibiting the development of any surface water flows. Therefore, the loess in the semi-arid and/or arid zones has not undergone significant disturbance and the AMS reliably reflects the paleowind direction, as many studies have suggested (e.g., Huang and Sun, 2005; Wu et al., 1998).

Recently, some authors (Zhang et al., 2010) suggested a new summer monsoon model for the generation of loess AMS based on their observation that the AMS of three loess sections in the west and central parts of Chinese Loess Plateau all show uniform SE–NW directions. They found that the direction of winter surface wind flow is much more variable than that of the summer wind flow and that the latter was rather consistent with the paleowind direction inferred from the AMS results. They concluded that although the sediment was transported to the area by the winter monsoon, the AMS was actually generated during the rainy summer monsoon season, when the wind direction was from the southeast, at which time the sedimentary particles were reoriented and locked in position. However, our results appear slightly different from their studies, for example, there are eight of the thirteen studied areas, i.e., Wudu, Xihe, Xining, Lanzhou, Dongwan, Lingtai, Luochuan, and Tongchuan, where the paleowind directions inferred by the loess AMS show a discrepancy with the summer wind directions but are almost consistent with that of the winter surface wind (Fig. 6), even though at the most southern sites of Xihe and Wudu the summer monsoon is much stronger. This seems to indicate that during the last glacial period the winter surface wind was the major factor determining the loess AMS in north China. Therefore, some more works on the generation of loess AMS, especially for loess of different ages and formed under different climatic conditions in China are still needed, such as the paleosols developed during the Quaternary interglacials and Neogene period.

Although the spatial resolution of the ECMWF ERA-Interim Reanalysis data is $0.75° × 0.75°$, significant differences between the Reanalysis data and the surface meteorological observation data can still be observed (Liu, 1998). The wind directions observed by the meteorological stations are much more variable and deviate significantly from the NW–SE and SE–NW directions (Liu, 1998), indicating constraints on the surface wind imposed by local topography. Therefore caution needs to be exercised when using the AMS of loess to infer the directions of East Asian monsoonal flow unless study sites are located in areas with an extensive flat surface and which are distant from mountains. However, since spatial variations of paleowind direction are significantly influenced by the regional topography, the AMS of Chinese loess can potentially be used to detect significant changes in past regional topography. For example, a wide range of observational evidence from its northeastern and eastern margins indicates that the Tibetan Plateau may have experienced major uplift in the late Cenozoic (Clark et al., 2005; Dupont-Nivet et al., 2008; Fang et al., 2005; Harrison et al., 1992; Lease et al., 2011; Métivier et al., 1998), and which has been suggested to cause significant changes in surface wind patterns (Dettman et al., 2003; Ge et al., 2013; Molnar, 2005). By studying the AMS of eolian deposits that have been dated back to the early Miocene or late Oligocene in north China (Guo et al., 2002; Qiang et al., 2011), and using the simulations of regional atmospheric circulation models, it may be possible to provide insights into the uplift history of the Tibetan Plateau.

5. Conclusions

In this paper we report the results of AMS measurements of loess of the last glacial period deposited at sites exhibiting varying slope angles in the Chinese Loess Plateau, in the West Qinling, and in the eastern margin of the Qilian Mountain. The results show that magnetic lineations are clustered along similar orientations in the same region regardless of differences in slope exposure and angle, but that significant differences in orientation are observed in different regions. This suggests that during the course of deposition of the eolian grains, air circulation rather than the surface water flow on the slope beds determines the direction of alignment of the magnetic mineral particles and consequently confirms the ability of the AMS to record the paleowind direction. In addition, by comparing the summer and winter surface wind patterns, we conclude that the AMS of Chinese loess is mainly determined by the regional surface wind flow that occurred during the course of dust accumulation, rather than by the large-scale atmospheric circulation. Finally, since wind direction is influenced significantly by the regional topography, the AMS of the Chinese loess–soil sequences, which have been dated back to the early Miocene, may have the potential to provide insights into significant changes of the past regional topography, especially the uplift of the Tibetan Plateau.

Acknowledgments

References

An, Z., Liu, T., Lu, Y., Porter, S.C., Kukla, G., Wu, X., Hua, Y., 1990. The long-term paleomonsoon variation recorded by the loess–paleosol sequence in Central China. Quat. Int. 7–8, 91–95.

An, Z.S., Kukla, G., Porter, S.C., Xiao, J.L., 1991. Late Quaternary dust flow on the Chinese Loess Plateau. Catena 18, 125–132.

Bradák, B., 2009. Application of anisotropy of magnetic susceptibility (AMS) for the determination of paleo-wind directions and paleo-environment during the accumulation period of Bag Tephra, Hungary. Quat. Int. 198, 77–84.

Chen, L.X., Zhu, Q.G., Luo, H.B., He, J.H., Dong, M., Feng, Z.Q., 1991. Monsoons Over East Asia (in Chinese)China Meteorological Press, Beijing.

Clark, M.K., House, M.A., Royden, L.H., Whipple, K.X., Burchfiel, B.C., Zhang, X., Tang, W., 2005. Late Cenozoic uplift of southeastern Tibet. Geology 33, 525–528.

Clarke, M.L., 1995. A comparison of magnetic fabrics from loessic silts across the Tibetan Front, Western China. Quat. Proc. 4, 19–26.

CLIMAP Project Members, 1976. The surface of the ice age earth. Science 191, 1131–1137.
Constable, C., Tauxe, L., 1990. The bootstrap for magnetic susceptibility tensors. J. Geophys. Res. Solid Earth (1978–2012) 95, 8383–8395.
Day, R., Fuller, M., Schmidt, V.A., 1977. Hysteresis properties of titanomagnetites: grain-size and compositional dependence. Phys. Earth Planet. Inter. 13, 260–267.
Dee, D.P., Uppala, S.M., Simmons, A.J., Berrisford, P., Poli, P., Kobayashi, S., Andrae, U., Balmaseda, M.A., Balsamo, G., Bauer, P., 2011. The ERA-Interim reanalysis: configuration and performance of the data assimilation system. Q. J. R. Meteorol. Soc. 137, 553–597.
Deng, C., Zhu, R., Verosub, K.L., Singer, M.J., Vidic, N.J., 2004. Mineral magnetic properties of loess/paleosol couplets of the central loess plateau of China over the last 1.2 Myr. J. Geophys. Res. 109, B01103. http://dx.doi.org/10.01029/2003jb002532.
Dettman, D.L., Fang, X.M., Garzione, C.N., Li, J.J., 2003. Uplift-driven climate change at 12 Ma: a long ¹⁸O record from the NE margin of the Tibetan plateau. Earth Planet. Sci. Lett. 214, 267–277.
Ding, Z.L., Liu, T.S., Rutter, N.W., Yu, Z.W., Guo, Z.T., Zhu, R.X., 1995. Ice-volume forcing of East Asian winter monsoon variations in the past 800,000 years. Quat. Res. 44, 149–159.
Ding, Z.L., Derbyshire, E., Yang, S.L., Yu, Z.W., Xiong, S.F., Liu, T.S., 2002. Stacked 2.6-Ma grain size record from the Chinese loess based on five sections and correlation with the deep-sea δ¹⁸O record. Paleoceanography 17, 5–21.
Dupont-Nivet, G., Dai, S., Fang, X.M., Krijgsman, W., Erens, V., Reitsma, M., Langereis, C., 2008. Timing and distribution of tectonic rotations in the northeastern Tibetan Plateau. Geol. Soc. Am. Spec. Pap. 444, 73–87.
Ellwood, B.B., 1984. Bioturbation: minimal effects on the magnetic fabric of some natural and experimental sediments. Earth Planet. Sci. Lett. 67, 367–376.
Fang, X.M., Yan, M.D., Van der Voo, R., Rea, D.K., Song, C.H., Pares, J.M., Gao, J.P., Nie, J.S., Dai, S., 2005. Late Cenozoic deformation and uplift of the NE Tibetan Plateau: evidence from high-resolution magnetostratigraphy of the Guide Basin, Qinghai Province, China. Bull. Geol. Soc. Am. 117, 1208–1225.
Fukuma, K., Torii, M., 1998. Variable shape of magnetic hysteresis loops in the Chinese loess–paleosol sequence. Earth Planets Space 50, 9–14.
Ge, J.Y., Guo, Z.T., Zhan, T., Yao, Z.Q., Deng, C.L., Oldfield, F., 2012. Magnetostratigraphy of the Xihe loess–soil sequence and implication for late Neogene deformation of the West Qinling Mountains. Geophys. J. Int. 189, 1399–1408.
Ge, J.Y., Dai, Y., Zhang, Z.S., Zhao, D.A., Li, Q., Zhang, Y., Yi, L., Wu, H.B., Oldfield, F., Guo, Z.T., 2013. Major changes in East Asian climate in the mid-Pliocene: triggered by the uplift of the Tibetan Plateau or global cooling? J. Asian Earth Sci. 69, 48–59.
Guo, Z.T., Fedoroff, N., An, Z.S., 1991. Genetic types of the Holocene soil and the Pleistocene paleosols in the Xifeng loess section in the central China. In: Liu, T.S. (Ed.), Loess, Environment and Global Change. Science Press, Beijing, pp. 93–111.
Guo, Z.T., Biscaye, P., Wei, L.Y., Chen, X.H., Peng, S.Z., Liu, T.S., 2000. Summer monsoon variations over the last 1.2 Ma from the weathering of loess–soil sequences in China. Geophys. Res. Lett. 27, 1751–1754.
Guo, Z.T., Ruddiman, W.F., Hao, Q.Z., Wu, H.B., Qiao, Y.S., Zhu, R.X., Peng, S.Z., Wei, J.J., Yuan, B.Y., Liu, T.S., 2002. Onset of Asian desertification by 22 Myr ago inferred from loess deposits in China. Nature 416, 159–163.
Hao, Q.Z., Guo, Z.T., 2005. Spatial variations of magnetic susceptibility of Chinese loess for the last 600 kyr: implications for monsoon evolution. J. Geophys. Res. 110, B12101. http://dx.doi.org/10.11029/12005JB003765.
Harrison, T.M., Copeland, P., Kidd, W.S.F., Yin, A.N., 1992. Raising Tibet. Science 255, 1663–1670.
Heller, F., Beat, M., Wang, J.D., Li, H.M., Liu, T.S., 1987. Magnetization and sedimentary history of loess in the central Loess Plateau of China. In: Liu, T.S. (Ed.), Aspects of Loess Research. China Ocean Press, Beijing, pp. 147–163.
Hrouda, F., 1993. Theoretical models of magnetic anisotropy to strain relationship revisited. Phys. Earth Planet. Inter. 77, 237–249.
Huang, X.G., Sun, J.M., 2005. Study of the magnetic fabrics in Chinese loess–paleosols since the last interglacial: implication of the paleowind direction (in Chinese with English abstract). Quat. Sci. 25, 516–522.
Hus, J., 2003. The magnetic fabric of some loess/palaeosol deposits. Phys. Chem. Earth A/B/C 28, 689–699.
Jelinek, V., 1981. Characterization of the magnetic fabric of rocks. Tectonophysics 79, T63–T67.
Kukla, G., 1987. Loess stratigraphy in central China. Quat. Sci. Rev. 6, 191–219.
Lagroix, F., Banerjee, S.K., 2002. Paleowind directions from the magnetic fabric of loess profiles in central Alaska. Earth Planet. Sci. Lett. 195, 99–112.
Lagroix, F., Banerjee, S.K., 2004. The regional and temporal significance of primary aeolian magnetic fabrics preserved in Alaskan loess. Earth Planet. Sci. Lett. 225, 379–395.
Lease, R.O., Burbank, D.W., Clark, M.K., Farley, K.A., Zheng, D.W., Zhang, H.P., 2011. Middle Miocene reorganization of deformation along the northeastern Tibetan Plateau. Geology 39, 359–362.
Liu, T.S., 1985. Loess and the Environment China Ocean Press, Beijing.
Liu, M.G., 1998. Atlas of Chinese Physical Geography China Map Publishing House.
Liu, T.S., Ding, Z.L., 1998. Chinese loess and the paleomonsoon. Annu. Rev. Earth Planet. Sci. 26, 111–145.

Liu, W.M., Sun, J.M., 2012. High-resolution anisotropy of magnetic susceptibility record in the central Chinese Loess Plateau and its paleoenvironment implications. Sci. China Ser. D Earth Sci. 55, 488–494.
Liu, X.M., Xu, T.C., Liu, T.S., 1988. The Chinese loess in Xifeng, II. A study of anisotropy of magnetic susceptibility of loess from Xifeng. Geophys. J. Int. 92, 349–353.
Liu, P., Jin, C.S., Zhang, S., Han, J.M., Liu, T.S., 2008. Magnetic fabric of early Quaternary loess–paleosols of Longdan Profile in Gansu Province and the reconstruction of the paleowind directions. Chin. Sci. Bull. 53, 1450–1452.
Liu, W., Wang, J.L., Liu, Y.M., 2013. Magnetic fabrics of Daluliang loess and the paleowind direction indicated. J. Yunnan Normal Univ. 23, 64–69.
Lu, Y.C., Wang, X.L., Wintle, A.G., 2007. A new OSL chronology for dust accumulation in the last 130,000 yr for the Chinese Loess Plateau. Quat. Res. 67, 152–160.
Métivier, F., Gaudemer, Y., Tapponnier, P., Meyer, B., 1998. Northeastward growth of the Tibet plateau deduced from balanced reconstruction of two depositional areas: the Qaidam and Hexi Corridor basins, China. Tectonics 17, 823–842.
Mock, C.J., Bartlein, P.J., Anderson, P.M., 1998. Atmospheric circulation patterns and spatial climatic variations in Beringia. Int. J. Climatol. 18, 1085–1104.
Molnar, P., 2005. Mio-Pliocene growth of the Tibetan Plateau and evolution of East Asian climate. Palaeontol. Electron. 8, 1–23.
Nawrocki, J., Polechońska, O., Boguckij, A., Łanczont, M., 2006. Palaeowind directions recorded in the youngest loess in Poland and western Ukraine as derived from anisotropy of magnetic susceptibility measurements. Boreas 35, 266–271.
Qiang, X., An, Z., Song, Y., Chang, H., Sun, Y., Liu, W., Ao, H., Dong, J., Fu, C., Wu, F., 2011. New eolian red clay sequence on the western Chinese Loess Plateau linked to onset of Asian desertification about 25 Ma ago. Sci. China Ser. D Earth Sci. 54, 136–144.
Rees, A.I., 1966. The effect of depositional slopes on the anisotropy of magnetic susceptibility of laboratory deposited sands. J. Geol. 74, 856–867.
Rees, A.I., Von Rad, U., Shepard, F.P., 1968. Magnetic fabric of sediments from the La Jolla submarine canyon and fan, California. Mar. Geol. 6, 145–150 (155–163, 167–178).
Robin, P.-Y.F., Jowett, E.C., 1986. Computerized density contouring and statistical evaluation of orientation data using counting circles and continuous weighting functions. Tectonophysics 121 (2–4), 207–223.
Sun, J.M., Ding, Z.L., Liu, T.S., 1995. Primary application of magnetic susceptibility measurement of loess and paleosols for reconstruction of winter monsoon direction. Chin. Sci. Bull. 40, 1976–1978.
Sun, D.H., Wu, X.H., Liu, T.S., 1996. Evolution of the summer monsoon regime over the Loess Plateau of the last 150 ka. Sci. China Ser. D Earth Sci. 39, 503.
Tarling, D.H., Hrouda, F., 1993. The Magnetic Anisotropy of Rocks Springer, London.
Thistlewood, L., Sun, J.Z., 1991. A palaeomagnetic and mineral magnetic study of the loess sequence at Liujiapo, Xian, China. J. Quat. Sci. 6, 13–26.
Wang, J.L., Fang, X.M., Zhang, Y.T., Cao, J.X., 1995. The anisotropy of loess magnetic susceptibility in the northeastern fringe of Qinghai–Xizang (Tibetan) Plateau as and indicator of paleowind direction. J. Lanzhou Univ. (Nat. Sci. Ed.) 31, 155–159.
Wang, Y., Pan, B.T., Gao, H.S., Guan, Y.Q., Chen, Y.Y., Wang, J.P., 2007. Magnetic fabric based reconstruction of the paleowind direction from a loess sequence in the northeastern flank of the Qilian Mountains. Chin. J. Geophys. 50, 1161–1166.
Wu, H.N., Yue, L.P., 1997. The anisotropy of magnetic susceptibility of aeolian dust sediment: the paleowind field in Chinese Loess Plateau. Acta Geophys. Sin. 40, 487–494.
Wu, H.B., Chen, F.H., Wang, J.M., Cao, J.X., Zhang, Y.T., 1998. A study on the relationship between magnetic anisotropy of modern eolian sediments and wind direction. Acta Geophys. Sin. 41, 811–817.
Yang, S.L., Ding, Z.L., 2008. Advance–retreat history of the East-Asian summer monsoon rainfall belt over northern China during the last two glacial–interglacial cycles. Earth Planet. Sci. Lett. 274, 499–510.
Zhang, Y.T., Chen, F.H., Cao, J.X., Li, Z., Ma, H.Z., 1993. A preliminary study on the anisotropy of magnetic susceptibility of Chinese loess. J. Lanzhou Univ. (Nat. Sci.) 29, 168–169.
Zhang, R., Kravchinsky, V.A., Zhu, R.X., Yue, L.P., 2010. Paleomonsoon route reconstruction along a W–E transect in the Chinese Loess Plateau using the anisotropy of magnetic susceptibility: summer monsoon model. Earth Planet. Sci. Lett. 299, 436–446.
Zhong, W., Fang, X.M., Cao, J.X., Wang, J.L., 1996. Study on the magnetic fabric features of the samples taken from Dongshanding profile in Linxia Basin, Gansu Province. J. Lanzhou Univ. (Nat. Sci.) 32, 116–120.
Zhu, R.X., 2000. History of anisotropy of the magnetic susceptibility and its implications: preliminary results along an EW transect of the Chinese Loess Plateau. Geophys. Res. Abstr. 2, 226.
Zhu, R., Liu, Q., Jackson, M.J., 2004. Paleoenvironmental significance of the magnetic fabrics in Chinese loess–paleosols since the last interglacial (<130 ka). Earth Planet. Sci. Lett. 221, 55–69.
Zhu, Y.M., Zhou, L.P., Zhang, S.H., 2007. A preliminary study on anisotropy of magnetic susceptibility of the late Pliocene–early Pleistocene aeolian deposits in Northern China (in Chinese with English abstract). Quat. Sci. 27, 1009–1014.